

Key Points:

- Dissolved organic nitrogen (DON) and dissolved inorganic nitrogen exhibited dissimilar distributions in a subtropical river-dominated estuary
- Physical mixing and biological activities promoted DON retention in the freshwater-seawater mixing zone
- Freshwater discharge mainly affected DON distribution in the main estuary

Supporting Information:

Supporting Information may be found in the online version of this article.

Correspondence to:

X. Huang and Y. Wu,
xphuang@scsio.ac.cn;
wuyunchao@scsio.ac.cn

Citation:

Li, J., Wu, Y., Jiang, Z., Liu, S., Ren, Y., Yang, J., et al. (2023). Terrestrial and biological activities shaped the fate of dissolved organic nitrogen in a subtropical river-dominated estuary and adjacent coastal area. *Journal of Geophysical Research: Oceans*, 128, e2023JC019911. <https://doi.org/10.1029/2023JC019911>






Received 7 APR 2023

Accepted 9 NOV 2023

Author Contributions:

Conceptualization: Jinlong Li
Funding acquisition: Xiaoping Huang
Investigation: Jinlong Li, Yunchao Wu, Zhijian Jiang, Songlin Liu, Yuzheng Ren, Jia Yang
Methodology: Jinlong Li, Yunchao Wu, Zhijian Jiang
Resources: Yuzheng Ren, Jia Yang, Xingyu Song
Software: Xingyu Song
Supervision: Xiaoping Huang
Visualization: Songlin Liu
Writing – original draft: Jinlong Li
Writing – review & editing: Yunchao Wu, Xiaoping Huang, Ding He

Terrestrial and Biological Activities Shaped the Fate of Dissolved Organic Nitrogen in a Subtropical River-Dominated Estuary and Adjacent Coastal Area

Jinlong Li^{1,2,3,4}, Yunchao Wu^{1,2,3} , Zhijian Jiang^{1,2,3,4} , Songlin Liu^{1,2,3,4}, Yuzheng Ren^{1,2,3,4} , Jia Yang^{1,2,3,4}, Xingyu Song^{1,4,5}, Xiaoping Huang^{1,2,3,4} , and Ding He⁶ 

¹Key Laboratory of Tropical Marine Bio-Resources and Ecology, South China Sea Institute of Oceanology, Chinese Academy of Sciences, Guangzhou, China, ²Southern Marine Science and Engineering Guangdong Laboratory (Guangzhou), Guangzhou, China, ³Guangdong Provincial Key Laboratory of Applied Marine Biology, Guangzhou, China, ⁴University of Chinese Academy of Sciences, Beijing, China, ⁵Nansha Marine Ecological and Environmental Research Station, South China Sea Institute of Oceanology, Chinese Academy of Sciences, Guangzhou, China, ⁶Department of Ocean Science, Hong Kong Branch of the Southern Marine Science and Engineering Guangdong Laboratory (Guangzhou), The Hong Kong University of Science and Technology, Hong Kong, China

Abstract Estuaries are key areas for terrestrial material transport and marine biogeochemical processes, particularly those of dissolved inorganic nitrogen (DIN) and dissolved organic nitrogen (DON). However, the fate of DON in estuaries with a high runoff remains poorly understood. In this study, we explored the translocation and transformation of DON in the Pearl River Estuary (PRE) and adjacent coastal areas of southern China based on DON concentrations, optical and fluorescence characteristics, and environmental parameters. The results revealed that DIN and DON exhibited dissimilar distributions. The distribution of DIN was primarily influenced by freshwater-seawater mixing. In contrast, biological processes and freshwater-seawater mixing shaped the distribution of DON. High levels of DON in the terrestrial-dominated zone were predominantly anthropogenic sources through terrestrial inputs, whereas DON in the freshwater-seawater mixing zone and seawater-based zone were mainly influenced by biological activities, as high concentrations of *Chla* were observed in these two areas. DON exhibits fast dilution in low-salinity areas and retention in moderate-salinity areas (freshwater-seawater mixing area) in summer and winter, while undergoes a rapid decrease in open water areas during winter. Consequently, DON in the PRE and adjacent coastal areas exhibited nonconservative mixing despite seasonal variations. These findings provide novel insights into the role of DON in nitrogen biogeochemical processes in river-dominated estuaries and adjacent coastal areas.

Plain Language Summary Physical and biological mechanisms affect the fate of dissolved organic nitrogen (DON) in estuaries and coastal waters. The results revealed that dissolved inorganic nitrogen (DIN) and DON exhibited dissimilar distributions. Freshwater discharge governed DON in areas dominated by terrestrial inputs, whereas biological activities shaped the DON fate in less affected areas. Increasing phytoplankton-derived autochthonous DON triggered by terrestrial inputs and seawater intrusion jointly promoted DON retention in brackish waters. This study shed light on how terrestrial inputs and biological activities shape DON dynamics in distinct areas, contributing to a deeper understanding of nitrogen cycling in high-runoff estuaries.

1. Introduction

Estuaries, which connect continents and oceans, are among the most productive, resourceful, and dynamic aquatic ecosystems in coastal regions (Bianchi & Allison, 2009; Paerl, 2006). This vast area experiences the most intensive human activities, making them highly dynamic and complex regions (M. Cai et al., 2016; Cloern et al., 2016; Rabouille et al., 2001). These areas are characterized by rapid nutrient utilization and transformation, particularly in estuaries with significant runoff and human activity (Boynton et al., 1995; K. Wu et al., 2017). Consequently, substantial quantities of nutrients from terrestrial sources enter coastal water. These nutrients are transported, mixed, and utilized during freshwater and seawater mixing processes, particularly in estuaries with high net flows and human population densities (F.-H. Lu et al., 2009; B. Wang, Ming, Wei, & Xie, 2018).

Nitrogen represents the largest pool of actively cycled nutrients in the ocean (Galloway et al., 2003). Dissolved inorganic nitrogen (DIN) is an essential nutrient for marine organisms and has caused ecological and environmental issues (e.g., eutrophication and pollution) in estuaries, as indicated by in-depth reports (Huang et al., 2003; McClelland & Valiela, 1998; Statham, 2012). While DIN has attracted much attention in coastal waters, mainly because of its high bioavailability and association with anthropogenic pollution (McCallum et al., 2021), less concern has been raised regarding DON owing to its complex composition. Recent studies have shown that DON is an important component of aquatic N pools and plays a crucial role in regulating N cycling and primary production in marine ecosystems (Bradley et al., 2010; Bronk et al., 2007; Zhang et al., 2022). Notably, DON dominates total dissolved nitrogen (TDN) in the open ocean and accounts for nearly half of the TDN in estuaries and coastal waters (D. Lu et al., 2016; Sipler & Bronk, 2015; Worsfold et al., 2008).

Despite the crucial role of DON in global biogeochemical cycles, characterization of its distribution regimes and sources in coastal waters remains challenging. Hydrological and biological processes influence the chemical fate and dynamics of organic nitrogen species in estuaries and coastal environments (Harrison et al., 2008). Meanwhile, DON comprises a range of highly labile and semi-labile compounds (e.g., urea and amino acids) that have a relatively rapid turnover and refractory components (e.g., amides and humic-like substances) that persist in water for years (Berman & Bronk, 2003; Bronk et al., 2007). Additionally, DON accumulation may trigger negative effects in coastal waters, including hypoxia, harmful algal blooms, and eutrophication (Bronk, 2002; Geeraert et al., 2021; Glibert et al., 2006; Lusk & Toor, 2016).

DON in estuaries and coastal waters is derived from various sources, for example, allochthonous (rivers, ground-water, and atmospheric deposition) and autochthonous (phytoplankton, N₂ fixers, bacteria, viruses, microzooplankton, and macrozooplankton) sources (Berman & Bronk, 2003; Sipler & Bronk, 2015). In addition, anthropogenic activities greatly affect coastal water quality by introducing excess nitrogen into rivers (Pennino et al., 2016; Stokral et al., 2017). The composition and structure of DON differ among variable sources (Y. Li et al., 2019; Petrone et al., 2008). As a major fraction of dissolved organic matter (DOM), DON is in line with dissolved organic carbon (DOC) in coastal waters (Hildebrand et al., 2022; Lee et al., 2020). This synergistic change enables the characterization of DON using similar techniques, such as ultraviolet-visible (UV-vis) adsorption spectroscopy and the emission-excitation matrix combined with parallel factor analysis (EEM-PARAFAC), to explore its composition and distinguish its sources (Osburn et al., 2016; L. Wang et al., 2021).

DIN dynamics in coastal areas have been fully explored and are comprehensively understood (Furtula et al., 2012; Ke et al., 2022; M. Wu et al., 2016); however, few attempts have been made to determine the composition, source, and quantity of DON. Based on the different geochemical cycle processes of DIN, understanding the sources and fate of DON in estuaries and adjacent coastal areas help to better constrain the nitrogen cycle processes in coastal areas. Therefore, we selected a large nearshore estuary, the Pearl River Estuary (PRE), and its adjacent areas in southern China as the target area. The PRE and adjacent coastal waters receive bulk discharge from the largest river system (the Zhujiang River) in southern China, which shows active biological activities exerting idiosyncratic biogeochemical processes of organic nitrogen compared to that in the open ocean (Su, 2004; Q. Wang et al., 2021). In this study, we aim to: (a) determine the spatial distribution of DIN and DON in the coastal water column and the potential impact processes, (b) interpret the autochthonous DON during strong runoff and mixing processes, and (c) ascertain how strong river runoff and potential biological effects drive the DON dynamics and its distribution regime in coastal waters. This study will help reveal the organic nitrogen biogeochemical processes and provide new insights into nitrogen dynamics in large estuarine areas with strong human disturbance and runoff input.

2. Materials and Methods

2.1. Sample Collection

This study was conducted in the PRE and adjacent coastal area (21.30°–22.73°N, 113.09°–114.94°E, Figure 1) (see detailed site description in the supplementary material). Water samples were collected during two cruises in July 2019 (summer) and January 2020 (winter) (Figure 1). Three typical transects were positioned from east to west in the PRE coastal waters. Transect A (hereafter referred to as TA) was in the middle of the Lingdingyang estuary and extended for 50 km, transect B (hereafter referred to as TB) was set from inner Daya Bay to 60 km away from the bay, and transect C (hereafter referred to as TC) was extended from the Huangmaohai Estuary to

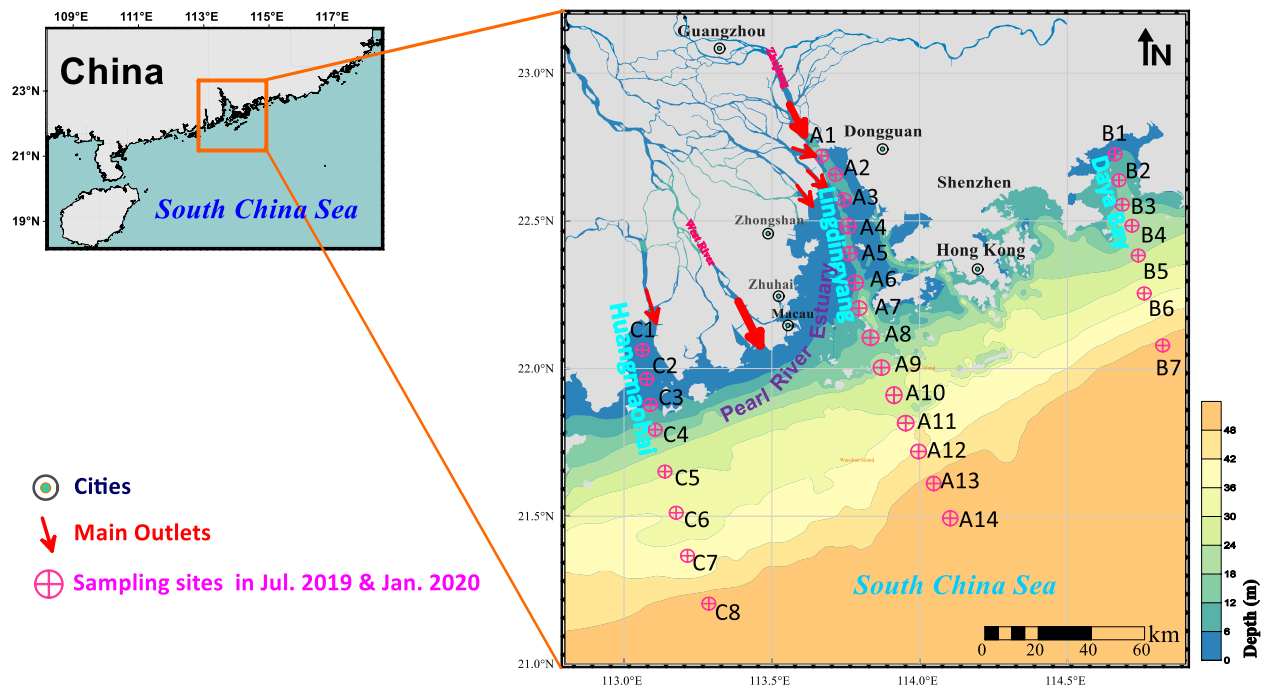


Figure 1. Bathymetric map displaying sampling stations in the Pearl River Estuary and adjacent coastal area during summer and winter cruises.

its adjacent sea area. A total of 29 sampling sites were designated, with 14 stations in TA, seven stations in TB, and eight stations in TC (for detailed information on the seawater column layers, see the Table S1 in Supporting Information S1).

Water samples were collected from the surface, middle, and bottom layers at each station using a 5 L Niskin bottle. The surface seawater samples were collected at a depth of 0.5 m; the bottom samples were collected at a depth of 2 m above the seabed; and 0–3 (e.g., 10, 20, and 30 m) middle samples were collected according to the bottom depth at each station. Seawater samples were immediately vacuum-filtered in the field using pre-combusted (450°C, 4 hr) glass-fiber filters (Whatman GF/F, 47 mm in diameter, 0.7 μm in pore size), and subsamples for subsequent analyses were preserved. All filtered samples were preserved in pre-cleaned polyethylene bottles and stored at −20°C until analysis. Environmental parameters including chlorophyll a (*Chla*) concentration, dissolved oxygen (DO), salinity (S), pH, water temperature (Temp), and turbidity (Turb), were measured in situ using a YSI profiler (RBR Brevio3, Canada).

2.2. Analytical Methods

TDN was measured using a high-temperature catalytic oxidation method using a total organic carbon (TOC) automatic analyzer (Shimadzu, TOC-VCPH-NML, Japan) equipped with a Total Nitrogen Module (detection limit = 0.002 mg N/L), with an accuracy of 2.3%. Reference samples of TDN (GBW(E)081020), national standard material by the Department of Water Ecology and Environment were measured every 10 samples to monitor accuracy. The DIN species, such as ammonia (NH_4^+), nitrate (NO_3^-), and nitrite (NO_2^-), were analyzed using an AA3 autoflow analyzer. The accuracies and recoveries of NH_4^+ and NO_2^- were better than 3.5% and 96.0%–103.2%, respectively. NO_3^- recovery was better than 90%. DIN was calculated as the sum of NH_4^+ , NO_3^- , and NO_2^- , and DON was calculated by subtracting DIN from TDN. The accuracy of DON detection was greater than 5.6%.

The UV-vis absorption spectra were recorded with a 3 cm quartz cuvette using a UV spectrophotometer (UV, Shimadzu, Japan) in the wavelength range of 220–800 nm. Baseline correction of the spectra was performed using ultrapure water. The spectra were corrected by subtracting the absorbance value at 700 nm. The spectral slopes at wavelengths from 275 to 295 nm ($S_{275-295}$) were used to determine the DON molecular weight (Helms et al., 2008).

Fluorescence EEMs were measured at an excitation (E_x) wavelength of 220–600 nm in 1 nm increments and an emission (E_m) wavelength of 230–450 nm in 2 nm increments using a fluorescence spectrophotometer. The scan rate was 12,000 nm/min. A blank sample of ultrapure water was measured each time, and the spectra were blank subtracted to remove the Raman scattering peak of water. The fluorescence intensity was converted into Raman units (R.U.) (Lawaetz & Stedmon, 2009). EEMs were used to calculate the humification index (HIX), biological index (BIX), and fluorescence index (FI). The HIX was calculated using Ex:Em at wavelength 254:435–480/254:300–345, BIX was calculated using Ex:Em at wavelength 310:380/310:430, and FI was calculated using Ex:Em at wavelength 370:450/370:500 (Fellman et al., 2010; Xie et al., 2018). To define the different components of DON, a PARAFAC (see details in the Figure S1 in Supporting Information S1) was conducted based on the corrected EEMs (Stedmon et al., 2003).

2.3. Conservative Mixing Model

In a large river-discharge estuary system, the theoretical dissolved inorganic and organic nitrogen concentrations from conservative mixing (N_{mix}) between river water and seawater could be calculated by applying a two-endmember conservative mixing model (Equation 1) (Middelburg & Nieuwenhuize, 2001):

$$N_{\text{mix}} = q \times N_f + (1 - q) \times N_s \quad (1)$$

where N_f and N_s refer to the dissolved inorganic and organic nitrogen concentrations of freshwater (samples with the lowest salinity [0.20 PSU in summer and 11.01 PSU in winter]) and seawater end-members (samples with the highest salinity [34.55 PSU in summer and 34.30 PSU in winter]), respectively; q is the fraction of freshwater, which is calculated from the salinities as follows (Equation 2):

$$q = (S_s - S_{\text{mix}}) / (S_s - S_f) \quad (2)$$

where S_s , S_f , and S_{mix} are the salinities of the seawater, freshwater, and sample water, respectively.

2.4. Data Process and Statistical Analysis

PARAFAC analysis was performed on the EEM data acquired from all the seawater samples using the drEEM 0.6.0 toolbox (Murphy et al., 2011). Detailed information about PARAFAC is available in Stedmon and Bro (2008) and Supporting Information S1.

The sampling map was plotted using Surfer 16.0. The nutrient distribution profiles were plotted using Ocean Data View (version 5.2.0). Pearson's correlation analysis was performed using the pheatmap and ggplot2 packages in R (version 2021.09.1). All other statistical analyses were performed using IBM SPSS Statistics version 26. Statistical significance was defined as a level of significance less than 0.05 ($p < 0.05$). Redundancy analysis (RDA) was used to characterize the linkages between dissolved nitrogen species and physiochemical parameters in Canoco 5.0. Hierarchical clustering analysis (HCA) was used to distinguish the seawater samples. HCA was realized using Origin Pro 2022 with the Ward linkage rule combined with the squared Euclidean distance.

3. Results

3.1. Dissolved Organic Nitrogen Distribution

The PRE and its adjacent coastal waters receive significant amounts of anthropogenic nutrients from riverine sources. Under this circumstance, the DIN concentration in the water column varied substantially between 0.66 and 220.71 $\mu\text{mol/L}$ (Figure 2a). The average DIN concentration was 36.59 ± 48.18 and 35.74 ± 53.65 $\mu\text{mol/L}$ in wet summer and dry winter, respectively (Table S2 in Supporting Information S1). No significant difference in DIN concentration was observed between summer and winter (Figure 2a). NO_3^- (average: 30.12 ± 44.00 $\mu\text{mol/L}$) was the dominant form of DIN, followed by NH_4^+ (average: 4.46 ± 7.43 $\mu\text{mol/L}$) and NO_2^- (average: 1.57 ± 2.01 $\mu\text{mol/L}$). NO_3^- was higher in summer (average: 32.93 ± 45.47 $\mu\text{mol/L}$) than in winter (27.45 ± 42.39 $\mu\text{mol/L}$), while NH_4^+ was higher in winter (6.51 ± 9.75 $\mu\text{mol/L}$) than in summer (average: 2.27 ± 1.81 $\mu\text{mol/L}$) (Table S2 in Supporting Information S1). The highest DIN values (the highest value is 220.71 $\mu\text{mol/L}$) were found in the inner stations of TA during winter. The average of the surface and bottom DIN concentrations decreased progressively from nearshore to offshore at TA and TC, whereas TB showed relatively low DIN concentrations (Figures 3a and 3b). In terms of the vertical distribution, the concentration of DIN was

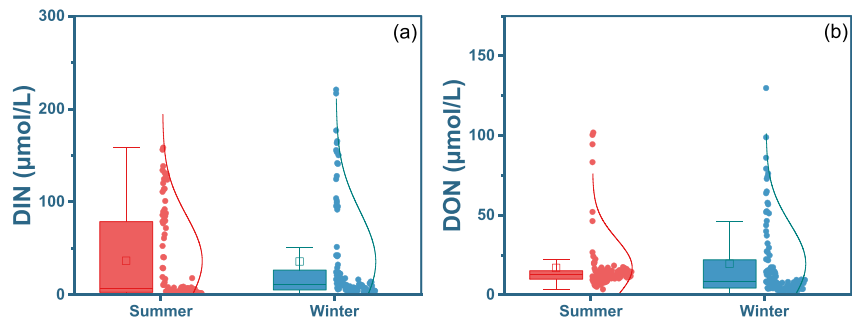


Figure 2. Concentrations of dissolved inorganic nitrogen (DIN) and dissolved organic nitrogen (DON) in all samples collected in summer and winter: (a) DIN and (b) DON.

generally higher in the surface waters of TA and TC during summer (Figures 4a and 4c). In winter, the DIN concentration was relatively homogeneous in the vertical section of the three transects, with higher values in the surface water of the inner stations in TA and TC (Figures 4g and 4i).

DON concentration varied from 0.98 to 129.80 µmol/L, displaying a narrower range than DIN (Table S2 in Supporting Information S1). DON accounted for $48.98\% \pm 27.10\%$ of TDN (Table S2 in Supporting Information S1), which was comparable to the contribution of DIN, indicating the important role of DON in nitrogen biogeochemical processes. The mean concentration of DON in summer (16.94 ± 18.09 µmol/L) was lower than that in winter (19.53 ± 25.01 µmol/L), though no significant difference was found between the two seasons (Figure 2b and Table S2 in Supporting Information S1).

DON showed heterogeneity and random distribution, with high values observed at the inner sites of TA and TC (Figures 3c and 3d), where the DIN concentration was also high. Notably, the highest DON values were observed

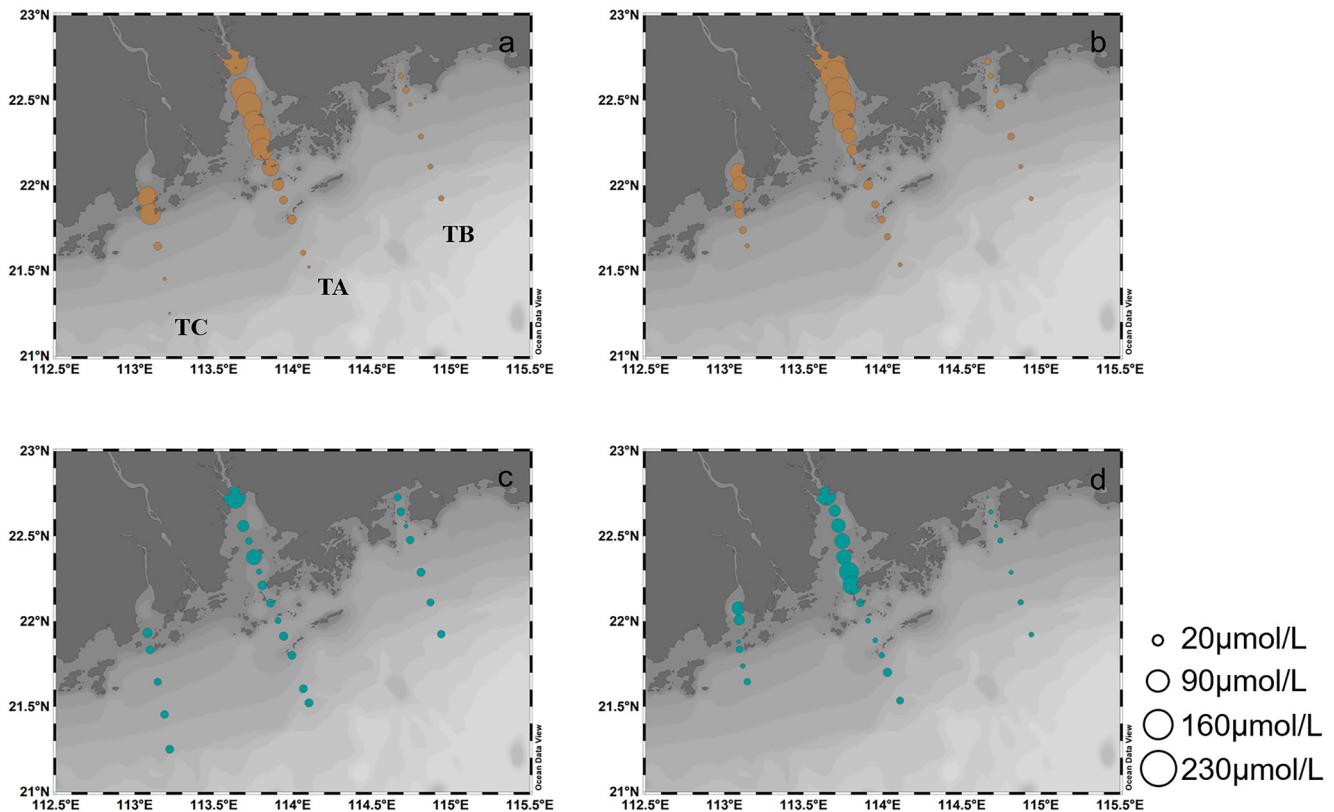


Figure 3. Horizontal distribution of the average of the surface and bottom dissolved nitrogen concentration: (a) dissolved inorganic nitrogen (DIN) in summer, (b) DIN in winter, (c) dissolved organic nitrogen (DON) in summer, (d) DON in winter.

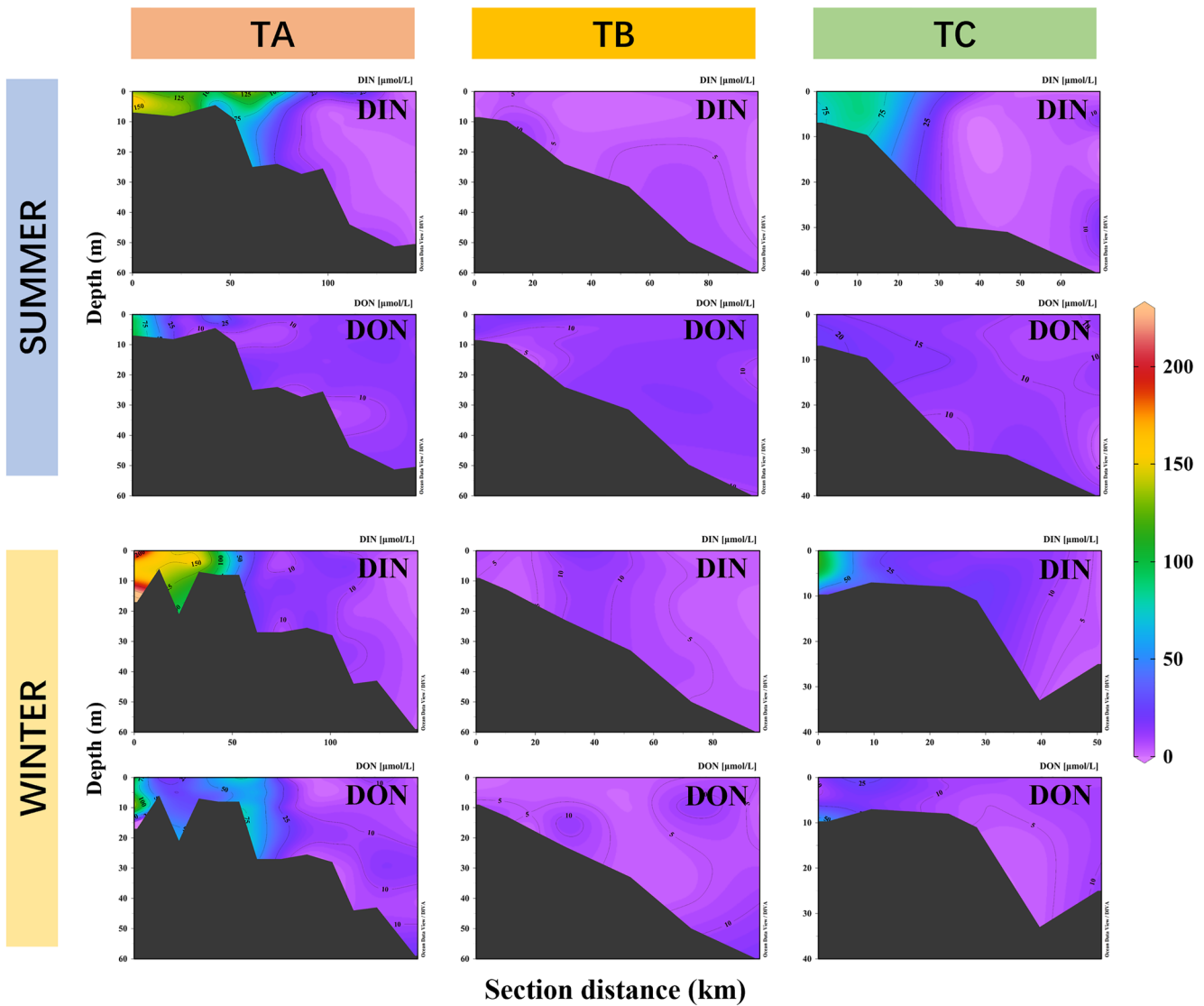


Figure 4. Vertical distribution of dissolved nitrogen: (a) dissolved inorganic nitrogen (DIN) in transect A (TA) in summer, (b) DIN in transect B (TB) in summer, (c) DIN in transect C (TC) in summer, (d) dissolved organic nitrogen (DON) in TA in summer, (e) DON in TB in summer, (f) DON in TC in summer, (g) DIN in TA in winter, (h) DIN in TB in winter, (i) DIN in TC in winter, (j) DON in TA in winter, (k) DON in TB in winter, (l) DON in TC in winter.

in the inner sites of the TA in winter; however, an increased DON concentration was found in the middle of the TA (Figure 3d). DON exhibited a similar distribution pattern at the outer stations in TA and TC and all stations in TB, with relatively low values observed at sites with high salinity (>30 PSU) (Figure 3 and Figure S2 in Supporting Information S1). The vertical distribution of DON in the PRE and adjacent coastal waters is shown in Figure 4. In general, the DON concentration was relatively higher in the surface water of the inner stations in TA and TC during summer, whereas it was patchily distributed in the rest of the area. In winter, the DON distribution was relatively homogeneous in the inner TA, whereas it was patchily distributed in the remaining zones.

3.2. DON in Different Regions

Water samples were classified into three categories based on HCA (Figure S3 in Supporting Information S1), representing three areas influenced by distinct degree of terrestrial inputs and human activities: the terrigenous-dominated zone (T zone), the freshwater-seawater mixing zone (M zone), and the seawater-based zone (S zone) (Figure S3 in Supporting Information S1). Stations in the three zones varied between seasons, indicating the divergent impact of human activities and terrestrial inputs (Table 1). The salinity yielded a gradient

Table 1
Average Concentrations of Dissolved N Species and Spectral Indices in Different Zones

Factors (units)	T			M			S		
	Summer	Winter	Total	Summer	Winter	Total	Summer	Winter	Total
S (PSU)	5.13 ± 4.54	16.34 ± 3.37	8.27 ± 6.59	25.46 ± 4.51	22.24 ± 2.44	23.45 ± 3.71	33.74 ± 1.27	32.82 ± 0.94	33.21 ± 1.18
Temp (°C)	28.22 ± 0.63	20.84 ± 0.17	26.16 ± 3.36	27.06 ± 1.79	20.17 ± 0.61	22.75 ± 3.54	25.49 ± 2.89	20.29 ± 0.88	22.50 ± 3.26
Chla (µg/L)	1.11 ± 0.62	1.21 ± 0.38	1.14 ± 0.57	2.44 ± 3.32	1.99 ± 7.53	2.16 ± 2.17	1.80 ± 2.44	1.45 ± 0.88	1.58 ± 1.65
DO (mg/L)	4.22 ± 1.20	6.61 ± 0.55	4.89 ± 1.51	4.63 ± 3.37	7.53 ± 0.37	6.44 ± 2.51	5.24 ± 1.39	7.39 ± 0.32	6.47 ± 1.41
pH	7.93 ± 0.20	7.60 ± 0.08	7.83 ± 0.23	8.25 ± 0.33	7.80 ± 0.03	7.97 ± 0.30	8.27 ± 0.13	8.07 ± 0.07	8.16 ± 0.14
Turb (FNU)	62.53 ± 74.68	13.00 ± 4.76	48.66 ± 67.20	12.87 ± 13.37	21.43 ± 17.45	18.21 ± 16.57	5.16 ± 14.66	3.27 ± 5.71	4.00 ± 10.19
DIN (µmol/L)	120.28 ± 20.88	178.84 ± 26.15	136.67 ± 34.60	58.78 ± 23.24	93.24 ± 41.21	80.32 ± 39.27	5.63 ± 7.04	10.63 ± 9.13	8.50 ± 8.67
DON (µmol/L)	31.41 ± 34.50	65.51 ± 37.62	40.96 ± 38.57	14.19 ± 5.09	31.25 ± 14.87	24.85 ± 14.70	11.92 ± 3.12	12.93 ± 19.07	12.50 ± 14.61
DON/TDN (%)	17.02% ± 12.56%	25.18% ± 11.11%	19.30% ± 12.71%	21.94% ± 11.09%	27.94% ± 15.44%	25.69% ± 14.27%	73.04% ± 19.62%	48.24% ± 21.80%	58.78% ± 14.27%
S ₂₇₅₋₂₉₅	0.020 ± 0.005	0.050 ± 0.000	0.018 ± 0.004	0.022 ± 0.007	0.020 ± 0.001	0.020 ± 0.004	0.041 ± 0.020	0.036 ± 0.012	0.038 ± 0.016
BIX	1.02 ± 0.06	1.36 ± 0.02	1.13 ± 0.16	1.20 ± 0.10	1.34 ± 0.06	1.28 ± 0.10	1.46 ± 0.22	1.27 ± 0.11	1.34 ± 0.19
HIX	0.45 ± 0.07	0.28 ± 0.07	0.40 ± 0.10	0.31 ± 0.10	0.32 ± 0.08	0.32 ± 0.09	0.17 ± 0.07	0.46 ± 0.10	0.34 ± 0.17
FI	2.31 ± 0.07	2.41 ± 0.06	2.34 ± 0.08	2.29 ± 0.06	2.37 ± 0.05	2.33 ± 0.07	2.30 ± 0.22	2.26 ± 0.25	2.27 ± 0.24

Note. T, M, and S indicate the terrigenous-dominated zone (T zone), freshwater-seawater mixing zone (M zone), and seawater-based zone (S zone), respectively.

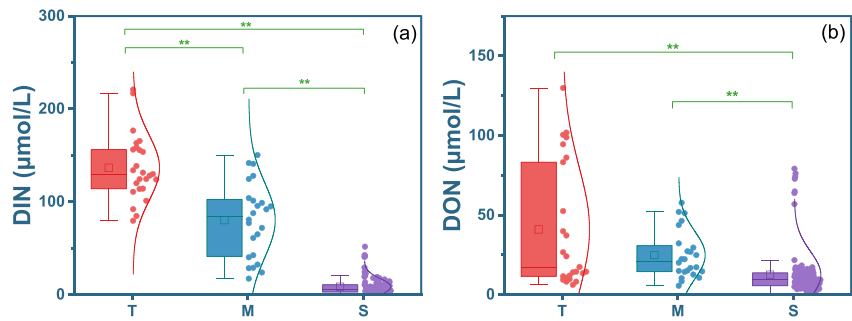


Figure 5. Comparisons of dissolved inorganic nitrogen (DIN) and dissolved organic nitrogen (DON) concentrations in three zones: (a) DIN and (b) DON. The p levels: ** $p < 0.01$; * $p < 0.05$; ns, not significant; T, T zone; M, M zone; S, S zone, similarly hereinafter.

from the T zone to the S zone (average: 8.27 ± 6.59 , 23.45 ± 3.71 , and 33.21 ± 1.18 PSU in the T, M, and S zones, respectively) (Table 1). In addition, the concentration of DIN differed significantly among the three zones ($p < 0.01$), with the highest mean value in the T zone ($136.67 \pm 34.60 \mu\text{mol/L}$), followed by the M zone ($80.31 \pm 39.28 \mu\text{mol/L}$) and S zone ($8.50 \pm 8.66 \mu\text{mol/L}$) (Figure 5a and Table 1). These findings indicate that terrestrial inputs had the greatest effect in the T zone and displayed a decreasing tendency in the M and S zones. The concentration of DON in the S zone ($40.96 \pm 38.57 \mu\text{mol/L}$) was significantly lower ($p < 0.05$) than that in the T zone ($24.85 \pm 14.70 \mu\text{mol/L}$) and the M zone ($12.50 \pm 14.60 \mu\text{mol/L}$), while no significant difference was observed between the T and M zones (Figure 5b and Table 1).

To identify the environmental factors contributing to the distribution of DIN and DON, *Chla*, DO, salinity, pH, and temperature were selected as environmental variables, whereas DIN and DON were defined as species for RDA. RDA1 and RDA2 explained 73.73% and 0.74% of the total variation, respectively, and the two RDA axes explained 74.47% (Figure 6). Salinity and pH settled in the negative RDA1, displayed an obvious negative correlation with water samples in the T zone, and were weakened in the M and S zones (Figure 6), indicating a weakened influence of river runoff on DON distribution from the T zone to the S zone. In addition, *Chla* and DO were two other environmental factors that influenced the DON distribution in the S zone, indicating the effect of biological activities.

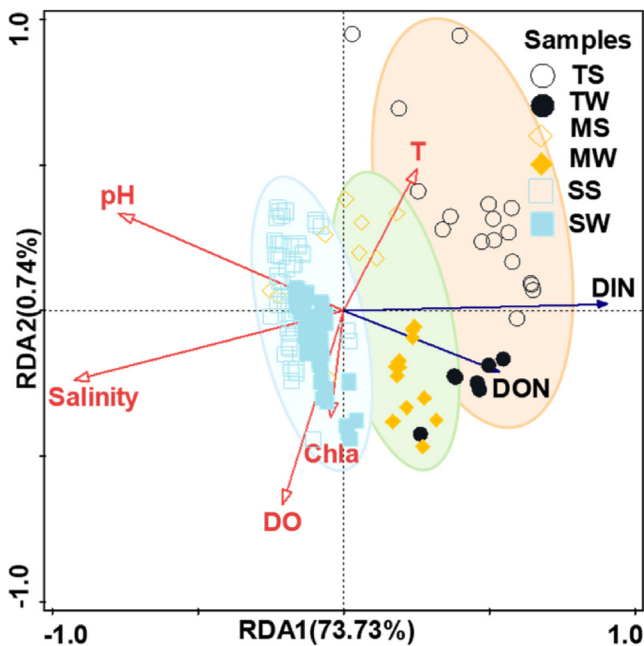


Figure 6. Hierarchical clustering analysis categories incorporate with redundancy analysis (RDA) triplot. (a) Black hollow cycles represent samples from the T zone in summer (TS); (b) black solid cycles represent samples from the T zone in winter (TW); (c) yellow hollow diamonds represent samples from the M zone in summer (MS); (d) yellow solid diamonds represent samples from M zone in winter (MW); (e) blue hollow squares represent samples from S zone in summer (SS); (f) blue solid squares represent samples from S zone in winter (SW). The red T in the figure represents temperature.

3.3. Correlations of DON With Fluorescence Components

Regarding DON as N-containing DOM, the relationship among the fluorescence intensities of DOM components ($F_{\text{max}1}$ to $F_{\text{max}6}$; see Supporting Information S1), concentrations of DIN and DON, and key environmental parameters (temperature, DO, *Chla*, and salinity) was revealed (Figure 7 and Figure S4 in Supporting Information S1). The results showed that $F_{\text{max}1}$ was significantly correlated with *Chla* ($p < 0.05$), whereas $F_{\text{max}2}$, $F_{\text{max}4}$, and $F_{\text{max}5}$ were significantly negatively correlated with salinity ($p < 0.001$, $p < 0.05$, and $p < 0.001$, respectively) (Figure 7a). In contrast, $F_{\text{max}3}$ and $F_{\text{max}6}$ were significantly positively correlated with salinity ($p < 0.05$ and $p < 0.001$, respectively) (Figure 7a). Mantel's analysis revealed that DIN was significantly negatively correlated with salinity ($p < 0.01$), indicating a strong terrestrial control of the DIN concentration. However, DON was slightly influenced by terrestrial inputs and $F_{\text{max}5}$ (algae-derived autochthonous fluorescence component, which was also found in the wastewater and aquaculture water) (Figure 7a).

In the T zone, DON exhibited no significant correlation with the fluorescence components (Figure 7b). In the M zone, DON was significantly correlated with $F_{\text{max}6}$ ($p < 0.01$) (Figure 7c), indicating autochthonous sources of

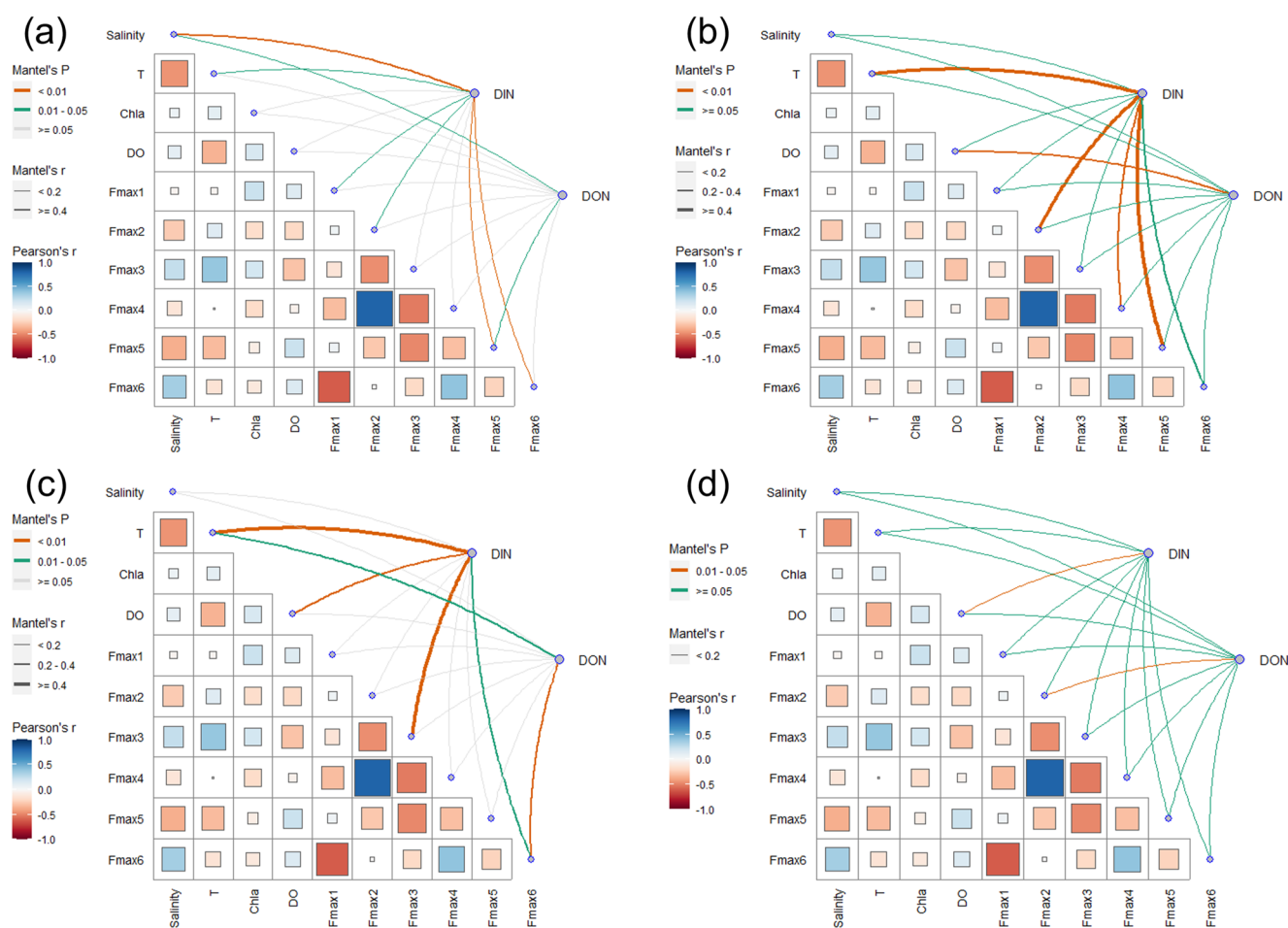


Figure 7. Correlations among fluorescence intensities of emission-excitation matrix components, dissolved inorganic nitrogen (DIN) and dissolved organic nitrogen (DON) concentrations, and key environmental parameters in (a) the Pearl River Estuary and adjacent coastal water, (b) the T zone, (c) the M zone, and (d) the S zone.

DON in this area. BIX, FI, and HIX in the M zone were 1.28 ± 0.10 , 2.33 ± 0.07 , and 0.32 ± 0.09 (Table 1 and Figure S5 in Supporting Information S1), respectively, further supporting a predominantly autochthonous origin for DON. In the S zone, DON was significantly correlated with $F_{\max 2}$ (Figure 7d). As indicated by the RDA results (Figure 6), DON was correlated with biological parameters such as *Chla* and DO in the S zone, suggesting a dominant autochthonous estuary origin in this area. Above all, DON in the T zone was mainly derived from terrestrial inputs, autochthonous production from freshwater algae, and C3 and C4 plants were secondary sources, while DON in the M and S zones was primarily derived from estuarine autochthonous production and was slightly influenced by terrestrial inputs.

3.4. Mixing Behavior of DIN and DON

As shown in Figure 8a, the DIN concentrations in the PRE and adjacent coastal areas were consistent with the DIN concentrations predicted by the two-end-member model in summer (slope = 0.98, $R^2 = 0.81$). In winter, the DIN mixing behavior was similar to that in summer (slope = 0.59, $R^2 = 0.85$). However, the dilution effect of seawater was not as intense as that in summer (the regression slope in summer and winter were 0.98 and 0.59, respectively), mainly because of the retention of nutrients in the inner estuary (TA and TC). However, the DON concentrations in the PRE and adjacent coastal areas deviated from those predicted by the two-end-member model in both seasons (Figure 8b), indicating nonconservative mixing behavior.

To better understand the fate and mixing law of DON along the salinity gradient in the PRE and adjacent coastal waters, regression statistical functions (best-fit regression with $p < 0.01$) were used to explore the dissipation

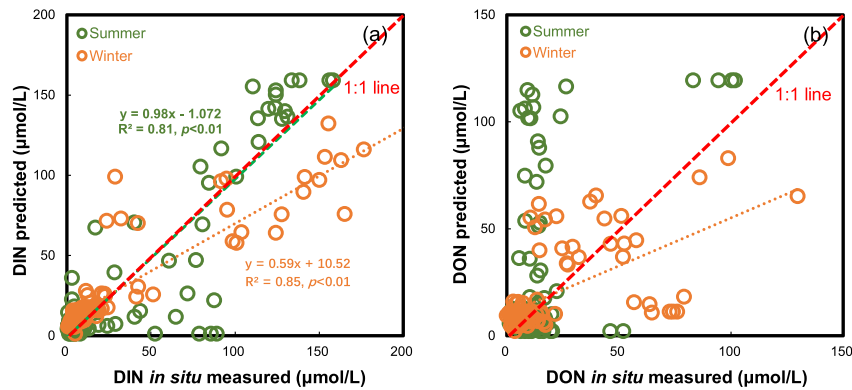


Figure 8. Predicted and in situ measured concentrations of dissolved inorganic nitrogen (DIN) (a) and dissolved organic nitrogen (DON) (b) using the two-endmember mixing model. The 1:1 line (red dashed line) is the modeled data for DIN and DON concentrations. A slope lower than 1:1 indicates a well-conservative mixing process. The green cycles represent summer samples, and the orange cycles represent winter samples.

patterns of DON and discuss the effects of biotic and abiotic impacts on the dissipation process, particularly during summer. By comparing the DON concentrations in summer and winter, it was observed that a large amount of terrestrial runoff input of nutrients in the flood season (i.e., summer) was negatively logarithmically dissipated ($y = -11.45\ln(x) + 49.57$, $R^2 = 0.64$, $p < 0.001$, Figure 9b). The most rapid DON dissipation occurred at the intersection of high-salinity, low-nutrient seawater and low-salinity, high-nutrient freshwater (i.e., upstream) affected by anthropogenic activities, indicating a rapid dilution effect of seawater on the nutrients in dilute water during the flood season. In contrast, DON concentrations in winter were the best cubic polynomial fitted and dissipated ($y = -0.031x^3 + 2.29x^2 - 56.23x + 494.12$, $R^2 = 0.41$, $p < 0.01$, Figure 9b). Notably, we observed a significant negative correlation between salinity and DIN concentration in both summer and winter seasons, suggesting distinct dilution processes of DIN when high freshwater inputs mix with seawater, primarily influenced by conservative mixing until the flushing water diminishes at salinities ranging from 33 to 35 PSU.

4. Discussion

4.1. Dissimilar Distribution of DON and DIN

The PRE and adjacent coastal waters (particularly in TA and TC in this study) are characterized as river input-dominated areas with significant freshwater inputs (3.5×10^{11} m³ annual discharge) (X. Wang et al., 2021). Anthropogenic, industrial, and agricultural activities contribute to the substantial nutrient loading in river outlets

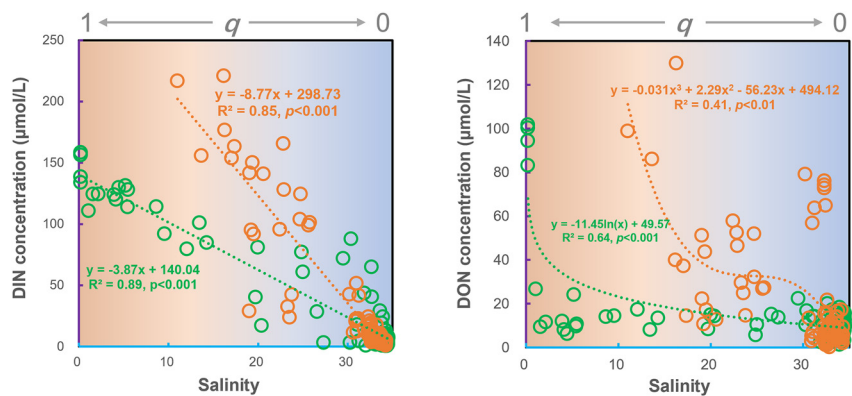


Figure 9. Runoff-induced seasonal distribution patterns of (a) dissolved inorganic nitrogen (DIN) and (b) dissolved organic nitrogen (DON) along the salinity gradient in the Pearl River Estuary and adjacent coastal waters. All data are best fitted for the regression analysis. Green circles represent nutrient species concentrations in summer, and orange circles represent that in winter. The dashed lines are the best-fitted regression line for nutrient species (the significant level is $p < 0.01$). The coefficient q at the top of the figure is the fraction of freshwater.

(red arrows in Figure 1) (Stokal et al., 2015). Consequently, the inner sites of the TA and TC exhibited high DIN and DON concentrations. DIN and DON concentrations surpass 100 $\mu\text{mol/L}$ in the Zhujiang River, particularly in areas influenced by strong terrestrial inputs or sewage discharge. The geostrophic deflection force also drove the transportation of DIN and DON from the Zhujiang River and major outlets (inner stations of the TA in Figure 1) to the inner sites of the TC. This phenomenon was covered in previous reports (Tao et al., 2021; M. Wu et al., 2016).

However, DIN and DON exhibited dissimilar distribution in TB and the outer sites in TA and TC, which were less influenced by terrestrial input. The inorganic nutrients required for nearshore phytoplankton and bacterial production mainly come from terrestrial inputs, and excessive inputs can result in algal blooms (R. H. et al., 2014; Y. Xu et al., 2019). Although inorganic nutrients are absorbed throughout these processes, a significant amount of organic nutrients is released. Consequently, DIN and DON exhibit dissimilar distributions (D. Lu et al., 2016; Y. Wang et al., 2012). This process is typically absent when newly discharged DIN and DON enter the estuary, particularly in the inner TA and TC sites, which have high turbidity and low plankton biomass. At the outer sites of TA and TC, the DIN concentration gradually decreased with increasing salinity (Figures 3a and 3b), whereas the DON concentration did not exhibit a clear trend. This indicates that the distribution of DIN is affected by the mixing process, whereas the distribution of DON may be affected by sophisticated biogeochemical processes (e.g., biological and photochemical activities) in addition to freshwater and seawater mixing (Bushaw et al., 1996; Grosse et al., 2019; Ianiri et al., 2022). Additionally, sufficient nutrients and high water transparency can stimulate phytoplankton growth (Rath et al., 2021), which in turn enhances the production of autochthonous DON. High *Chla* levels in the inner sites of the TB indicated active biological activity. A previous study found that the relative content of N-containing DOM molecules exhibited no clear trend as salinity increased within the PRE (He et al., 2020). This was probably due to autochthonous inputs. The high DON/TDN ratio in the TB further supported the impacts of biological activity. Overall, the biological activities induced dissimilar distributions of DIN and DON in areas where the terrestrial nutrient load was reduced.

4.2. Freshwater Discharge Governing DON Distribution in the Main Estuary

Continuous freshwater discharge during the rainy season (generally April to October in the Lingdingyang Estuary) plays an important role in facilitating the cross-boundary transportation of nutrients between terrestrial and marine environments (Niu et al., 2020; M. Wu et al., 2016; Ye et al., 2018). Nitrogen from allochthonous sources transported during these “hot moments” has the potential to significantly subsidize ecosystem metabolism (Z. Lu et al., 2018). As we focused on the main estuary of the PRE (Lingdingyang region, TA in Figure 1), an area that experiences drastic fluctuations due to complex human activities and estuary dynamic processes, the governing effect of freshwater on DON distribution was evident. First, a negative correlation between salinity and DON concentration was observed in TA (Figure S6 in Supporting Information S1), indicating a freshwater-governed distribution of DON. Second, TB, which has high salinity and low DON concentrations (Figure 4 and Table S1 in Supporting Information S1), appeared to be less affected by freshwater input. However, significantly higher DON concentrations at the inner sites of the TA (Figures 3c and 3d), suggest that freshwater discharge is crucial in affecting DON distribution. Furthermore, a substantial amount of freshwater ($2.8 \times 10^{11} \text{ m}^3$) flows from the Zhujiang River and is discharged into the PRE in the wet season (W.-J. Cai et al., 2004; Harrison et al., 2008), which significantly affects the salinity distribution and transportation of terrestrial nutrients, such as DIN, in the estuary. Consequently, salinity stratification prevailed in the TA during summer (Figure 10a). However, the concentration of DON rapidly decreased as freshwater was discharged into the estuary and remained at a relatively low concentration at the outer sites. In the dry season, the DON concentration was higher than that in the wet season, as reported in previous studies (Liu et al., 2020; Ye et al., 2018). This increase in DON concentration during the dry season (e.g., winter) could be attributed to reduced rainfall and diminished freshwater discharge, resulting in an extended residence time of DON in the estuary (Harrison et al., 2008). Additionally, the intrusion of saline seawater during winter was supported by a significant elevation in salinity levels in the inner estuary, which resulted in higher DON concentrations in the middle estuary (Figure 10b). Consequently, a considerable amount of terrestrial-origin DON was trapped within the salinity front (Figure 10b).

4.3. Autochthonous DON Increase in the Freshwater-Seawater Mixing Zone

Due to the diversity and bio-sensitivity of DON, identifying its sources in aquatic ecosystems can be challenging (Hansen et al., 2016). However, because DON is an N-containing component of DOM, its sources can be tracked

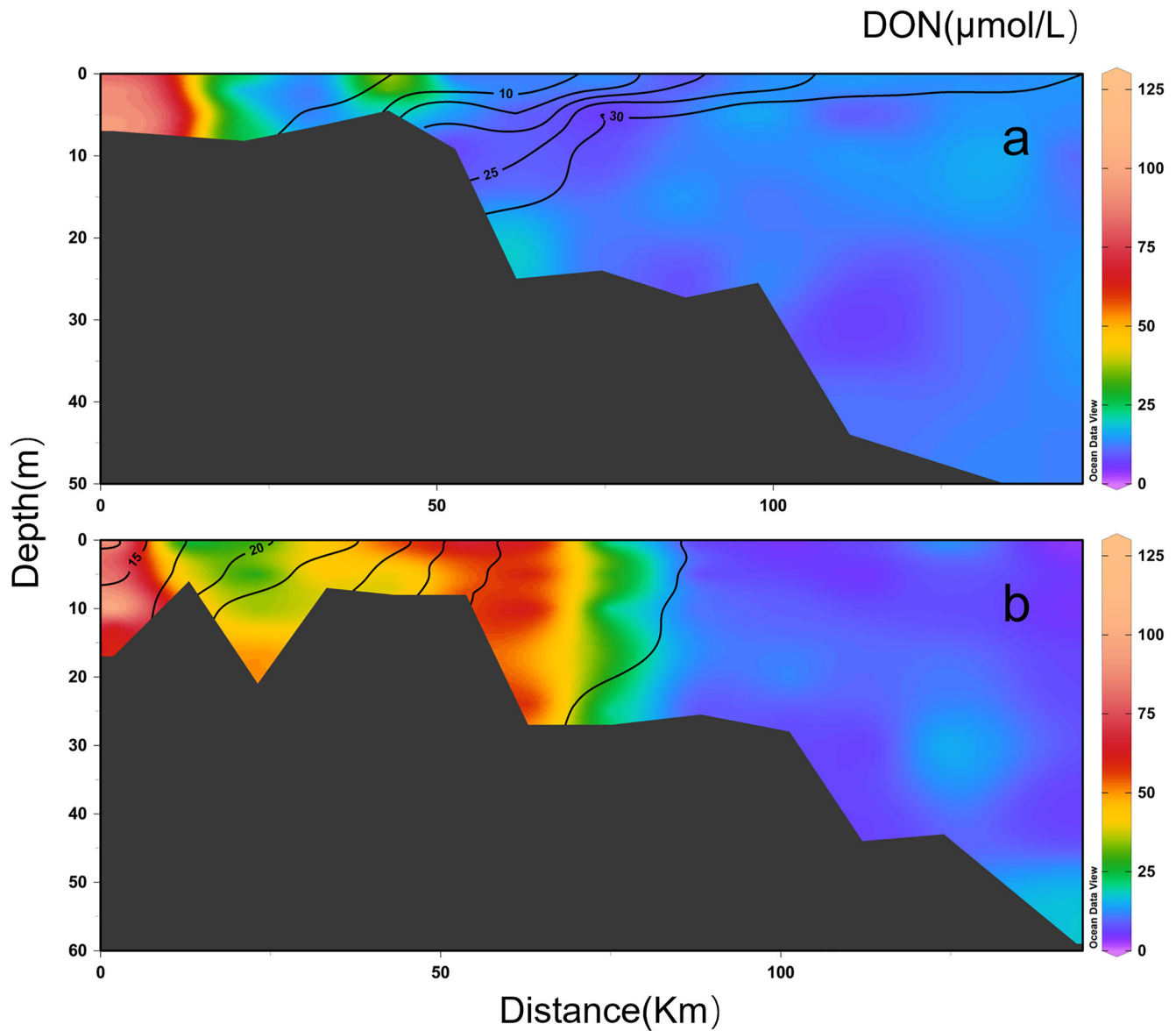


Figure 10. Vertical distribution of dissolved organic nitrogen (DON) and salinity in transect A: (a) in summer, (b) in winter. The colors in the plot represent DON concentrations and the contour lines demonstrate salinity distribution.

in a manner similar to that of DOM. Regarding the significant correlations between DON and the fluorescence intensities of DOM components (such as $F_{\max 5}$ in Figure 7), it is reasonable to infer the sources of DON in the PRE and adjacent coastal areas include wastewater, aquaculture waste, and autochthonous production (Table S3 in Supporting Information S1). The present study found that the BIX, FI, and HIX values ranged from 0.87 to 2.24, 1.61 to 2.86, and 0.04 to 0.65, respectively (Table S4 in Supporting Information S1), indicating that DON in the PRE and adjacent coastal waters originates from multiple sources, with a predominant contribution from autochthonous sources. This result is consistent with that reported by Xie et al. (2018), who identified autochthonous sources of DOC in the PRE based on the EEM results, despite the fact that terrestrial inputs are important sources of DOM in the upstream of the PRE (Meng et al., 2013).

The concentrations and characteristics (reflected by the fluorescence indices) of DON varied significantly across the three zones in the PRE and adjacent coastal waters (Table 1 and Figure 5), primarily owing to diverse sources and biogeochemical processes such as freshwater discharge, phytoplankton uptake, and hydrological mixing (D. Li et al., 2020; Qian et al., 2018). In the M zone, the correlation between DON and C6 (Figure 7c) and BIX and

C6 ($p < 0.01$) indicated that protein-like compounds were released. The increase in protein-like compounds in eutrophic aquatic ecosystems can be attributed to phytoplankton growth (e.g., priming effect). Excessive terrestrial nutrient inputs (including inorganic and organic forms) promote phytoplankton growth and trigger blooms (Jiang et al., 2015; Paerl, 1997). Notably, phytoplankton blooms (e.g., diatoms and *Synechococcus*) occasionally occurred in the M zone, as reported in previous studies (J. Li et al., 2019; Z. Lu & Gan, 2015; S. Xu et al., 2022). In the S zone, the correlation between DON and C2 (Figure 7d) likely indicates a terrestrial origin of DON. However, the DON concentration was relatively low, whereas the *Chla* concentration was relatively high in this area. Additionally, DON in the M and S zones was more bioavailable (with higher BIX than in the T zone; see Table 1), indicating that labile DON would be exuded due to phytoplankton provision or bacterial priming. Nitrogen-containing DOM components, including protein-like compounds, aliphatic compounds, and peptides produced from phytoplankton, contribute to the bioavailable DOM pool (Y. Zhou et al., 2021). A recent study showed that diatoms produce DON and promote bacteria growth in a river-dominated estuary (Ma et al., 2022). Moreover, previous studies have suggested that marine DOM is produced from phytoplankton and bacteria in the offshore area of the river-dominated Amazon River-to-ocean continuum (Medeiros et al., 2015; Seidel et al., 2015). The RDA result indicated that DON in the T zone could be inferred to be mainly derived from terrestrial sources (Figure 6), and there was no significant correlation between DON and fluorescence components in the T zone (Figure 7b). DON in the upstream areas may be derived from sewage during the dry season, whereas terrestrial organic matter is the major source of DON in the upper estuary during the wet season (Ye et al., 2018). Additionally, fluorescence indices, including BIX (1.36 ± 0.02), FI (2.34 ± 0.08), and HIX (0.40 ± 0.10) (Table 1) in the T zone, were in the range of an obvious terrestrial autochthonous origin (e.g., C3 plant, C4 plant, or freshwater algal) of DON. Therefore, we can conclude that the M and S zones were dominated by autochthonous DON, while the T zone was dominated by terrestrial DON.

4.4. DON Translocation Regimes in River-Discharge Estuaries

Coastal waters are among the most disturbed and receive large amounts of nutrients from anthropogenic sources through terrestrial inputs. Seasonal runoff in large river discharge estuary systems determines the effects of nutrients subject to traceable and regular dilution or dissipation characteristics in these areas (C. Wang, Lv, & Li, 2018; Ye et al., 2018). In these estuaries, the dilution of inorganic nutrients (M. Wu et al., 2016; Yan et al., 2019) and trace elements (X. Chen et al., 2021) during the strong freshwater-seawater mixing process is an expected event. However, in this study, the mixing behavior of DON was distinct from that of DIN, which was also reported by Ye et al. (2018) for the PRE. Conservative behavior for DON was not clearly observed, as evidenced by significant deviations between in situ DON concentrations and model-predicted values (1:1) (Figure 8b), particularly in low-salinity areas, presumably in response to stronger freshwater dilution or variability in DON sources. The predicted DON concentrations were significantly higher than those measured, indicating a rapid dilution rate. However, a pronounced retention phenomenon was observed at the moderate salinity (freshwater-seawater mixing area) (Figures 9 and 10). In addition to the interaction between seawater and freshwater, the conversion of nitrogen species is another factor that influences DON translocation. As reported by Dai et al. (2008), nitrification is the main DIN (mostly NO_3^-) removal process in the PRE. However, seawater's direct dilution effect is stronger than that of ammonification or nitrification. Reduced runoff input in winter weakened the estuarine hydrodynamic exchange rate and the apparent nonconservative mixing behavior of DON during moderate mixing ($0.25 < q < 0.55$). This nonconservative mixing behavior is more pronounced in areas affected by runoff input, such as the upper TA and TC, where higher DON concentrations also occurred during intensive mixing ($q \approx 0.10$) (top right in Figure 9b).

That needs to be verified further, which is why DON did not have rapid linear mixing, similar to DIN. DON can be produced by the release of living organisms or the decomposition of residues, which may cause differential behavior in coastal waters (Janiri et al., 2022; Liao et al., 2019). Coincidentally, the offshore phytoplankton and bacteria released a large amount of DON after entering the intersection area after 2 days of cultivation, with nearly five times the promotion of the proliferation of diatoms (the main algae species in the PRE and adjacent area) (Cheung et al., 2021). A similar result that episodic nutrient inputs may support increased phytoplankton and bacterial production was also found by N. Chen et al. (2018). Therefore, phytoplankton proliferation accelerates the release of DON (e.g., directly release, sloppy feeding by zooplankton, and lysis by viral infections) (Bronk, 2002; Z. Zhou et al., 2023). This goes a step further to explain why the DON concentration does not linearly decrease with DIN between the intersections at salinities of 20–30 PSU and exhibits a nonconservative mixing behavior.

In summary, our findings indicate that DON and DIN are differently distributed in the PRE and adjacent coastal waters. DIN imported through runoff from the Zhujiang River mainly dissipates in estuarine seawater, whereas DON exhibits a nonconservative mixing behavior. The mixing process of DON varies with seasons, with negative logarithmic mixing in low-salinity areas in summer, stable or rising stages in moderate salinity (16–26 PSU), and a rapid decline in areas dominated by open water (salinity higher than 33 PSU) in winter.

5. Conclusion

The DON and DIN in the PRE were dissimilarly dispersed via different mechanisms. Conservative mixing processes dominate DIN, whereas DON is affected by physical mixing and biological activities (i.e., nonconservative mixing behavior), and this process varies across seasons. In the terrestrial-dominated zone, the input of terrestrial materials from human activities causes high DON concentrations. In the freshwater-seawater mixing zone, terrestrial materials promote the growth of primary producers (including DIN assimilation and DON release), and DON is retained in the salinity fronts. In the seawater-based zone, DON concentrations are relatively low, with high biological activity, representing a dominant endogenous source of DON. This consequently led to source deviation in different physical mixing areas, terrestrial inputs in the terrigenous-dominated zone and the freshwater-seawater mixing and seawater-based zones from autochthonous production. In simple terms, the fate of DON is profoundly shaped by terrestrial and biological activities during transportation in the PRE and adjacent coastal areas.

Data Availability Statement

Research data in this study can be downloaded at <https://zenodo.org/record/8144290>.

Acknowledgments

This research was supported by Grants from the National Natural Science Foundation of China (NSFC, 41890852, 41906133, and U1901221), the Key Special Project for Introduced Talents Team of the Southern Marine Science and Engineering Guangdong Laboratory (Guangzhou) (GML2019ZD0405). This work was also supported by the Guangzhou Science and Technology Plan Project (202102021230) and Guangxi Key Laboratory of Beibu Gulf Marine Resources, Environment and Sustainable Development (MRES2023-A06). We also thank Yadong Huang of Nansha Marine Ecological and Environmental Research Station, South China Sea Institute of Oceanology for supporting the basic physiochemical data.

References

- Berman, T., & Bronk, D. A. (2003). Dissolved organic nitrogen: A dynamic participant in aquatic ecosystems. *Aquatic Microbial Ecology*, *31*, 279–305. <https://doi.org/10.3354/AME031279>
- Bianchi, T. S., & Allison, M. A. (2009). Large-river delta-front estuaries as natural “recorders” of global environmental change. *Proceedings of the National Academy of Sciences*, *106*(20), 8085–8092. <https://doi.org/10.1073/pnas.0812878106>
- Boynton, W. R., Garber, J. H., Summers, R., & Kemp, W. M. (1995). Inputs, transformations, and transport of nitrogen and phosphorus in Chesapeake Bay and selected tributaries. *Estuaries*, *18*(1), 285–314. <https://doi.org/10.2307/1352640>
- Bradley, P. B., Sandersen, M. P., Frischer, M. E., Brofft, J., Booth, M. G., Kerkhof, L. J., & Bronk, D. A. (2010). Inorganic and organic nitrogen uptake by phytoplankton and heterotrophic bacteria in the stratified Mid-Atlantic Bight. *Estuarine, Coastal and Shelf Science*, *88*(4), 429–441. <https://doi.org/10.1016/j.ecss.2010.02.001>
- Bronk, D. A. (2002). Dynamics of DON. In *Biogeochemistry of marine dissolved organic matter* (pp. 153–249). <https://doi.org/10.1016/B978-012323841-2/50007-5>
- Bronk, D. A., See, J. H., Bradley, P., & Killberg, L. (2007). DON as a source of bioavailable nitrogen for phytoplankton. *Biogeochemistry*, *4*(3), 283–296. <https://doi.org/10.1016/j.biogeochem.2007.04.001>
- Bushaw, K. L., Zepp, R. G., Tarr, M. A., Schulz-Jander, D., Bourbonniere, R. A., Hodson, R. E., et al. (1996). Photochemical release of biologically available nitrogen from aquatic dissolved organic matter. *Nature*, *381*(30), 4–407. <https://doi.org/10.1038/381404A0>
- Cai, M., Liu, Y., Chen, K., Huang, D., & Yang, S. (2016). Quantitative analysis of anthropogenic influences on coastal water—A new perspective. *Ecological Indicators*, *67*, 673–683. <https://doi.org/10.1016/j.ecolind.2016.03.037>
- Cai, W.-J., Dai, M., Wang, Y., Zhai, W., Huang, T., Chen, S., et al. (2004). The biogeochemistry of inorganic carbon and nutrients in the Pearl River estuary and the adjacent Northern South China Sea. *Continental Shelf Research*, *24*(12), 1301–1319. <https://doi.org/10.1016/j.csr.2004.04.005>
- Chen, N., Krom, M. D., Wu, Y., Yu, D., & Hong, H. (2018). Storm induced estuarine turbidity maxima and controls on nutrient fluxes across river-estuary-coast continuum. *Science of the Total Environment*, *628–629*, 1108–1120. <https://doi.org/10.1016/j.scitotenv.2018.02.060>
- Chen, X., Seo, H., Han, H., Seo, J., Kim, T., & Kim, G. (2021). Conservative behavior of terrestrial trace elements associated with humic substances in the coastal ocean. *Geochimica et Cosmochimica Acta*, *308*, 373–383. <https://doi.org/10.1016/j.gca.2021.05.020>
- Cheung, Y. Y., Cheung, S., Mak, J., Liu, K., Xia, X., Zhang, X., et al. (2021). Distinct interaction effects of warming and anthropogenic input on diatoms and dinoflagellates in an urbanized estuarine ecosystem. *Global Change Biology*, *27*(15), 3463–3473. <https://doi.org/10.1111/gcb.15667>
- Cloern, J. E., Abreu, P. C., Carstensen, J., Chauvaud, L., Elmgren, R., Grall, J., et al. (2016). Human activities and climate variability drive fast-paced change across the world's estuarine-coastal ecosystems. *Global Change Biology*, *22*(2), 513–529. <https://doi.org/10.1111/gcb.13059>
- Dai, M., Wang, L., Guo, X., Zhai, W., Li, Q., He, B., & Kao, S. J. (2008). Nitrification and inorganic nitrogen distribution in a large perturbed river/estuarine system: The Pearl River Estuary, China. *Biogeochemistry*, *5*(5), 1227–1244. <https://doi.org/10.5194/bg-5-1227-2008>
- Fellman, J. B., Hood, E., & Spencer, R. G. M. (2010). Fluorescence spectroscopy opens new windows into dissolved organic matter dynamics in freshwater ecosystems: A review. *Limnology & Oceanography*, *55*(6), 2452–2462. <https://doi.org/10.4319/lo.2010.55.6.2452>
- Furtula, V., Osachoff, H., Derksen, G., Juahir, H., Colodey, A., & Chambers, P. (2012). Inorganic nitrogen, sterols and bacterial source tracking as tools to characterize water quality and possible contamination sources in surface water. *Water Research*, *46*(4), 1079–1092. <https://doi.org/10.1016/j.watres.2011.12.002>
- Galloway, J. N., Aber, J. D., Erisman, J. W., Seitzinger, S. P., Howarth, R. W., Cowling, E. B., & Cosby, B. J. (2003). The nitrogen cascade. *BioScience*, *53*(4), 341–356. [https://doi.org/10.1641/0006-3568\(2003\)053\[0341:TNC\]2.0.CO;2](https://doi.org/10.1641/0006-3568(2003)053[0341:TNC]2.0.CO;2)

- Geeraert, N., Archana, A., Xu, M. N., Kao, S.-J., Baker, D. M., & Thibodeau, B. (2021). Investigating the link between Pearl River-induced eutrophication and hypoxia in Hong Kong shallow coastal waters. *Science of the Total Environment*, 772, 145007. <https://doi.org/10.1016/j.scitotenv.2021.145007>
- Glibert, P. M., Harrison, J., Heil, C., & Seitzinger, S. (2006). Escalating worldwide use of urea—A global change contributing to coastal eutrophication. *Biogeochemistry*, 77(3), 441–463. <https://doi.org/10.1007/s10533-005-3070-5>
- Grosse, J., Brussaard, C. P. D., & Boschker, H. T. S. (2019). Nutrient limitation driven dynamics of amino acids and fatty acids in coastal phytoplankton. *Limnology & Oceanography*, 64(1), 302–316. <https://doi.org/10.1002/lno.11040>
- Hansen, A. M., Kraus, T. E. C., Pellerin, B. A., Fleck, J. A., Downing, B. D., & Bergamaschi, B. A. (2016). Optical properties of dissolved organic matter (DOM): Effects of biological and photolytic degradation. *Limnology & Oceanography*, 61(3), 1015–1032. <https://doi.org/10.1002/lno.10270>
- Harrison, P. J., Yin, K., Lee, J. H. W., Gan, J., & Liu, H. (2008). Physical–biological coupling in the Pearl River Estuary. *Continental Shelf Research*, 28(12), 1405–1415. <https://doi.org/10.1016/j.csr.2007.02.011>
- He, C., Pan, Q., Li, P., Xie, W., He, D., Zhang, C., & Shi, Q. (2020). Molecular composition and spatial distribution of dissolved organic matter (DOM) in the Pearl River Estuary, China. *Environmental Chemistry*, 17(3), 240. <https://doi.org/10.1071/en19051>
- Helmis, J. R., Stubbins, A. D., Ritchie, J. C., Minor, E. J., Kieber, D., & Mopper, K. (2008). Absorption spectral slopes and slope ratios as indicators of molecular weight, source, and photobleaching of chromophoric dissolved organic matter. *Limnology & Oceanography*, 53(3), 955–969. <https://doi.org/10.4319/lno.2008.53.3.0955>
- Hildebrand, T., Osterholz, H., Bunse, C., Grotheer, H., Dittmar, T., & Schupp, P. J. (2022). Transformation of dissolved organic matter by two Indo-Pacific sponges. *Limnology & Oceanography*, 67(11), 2483–2496. <https://doi.org/10.1002/lno.12214>
- Huang, X. P., Huang, L. M., & Yue, W. Z. (2003). The characteristics of nutrients and eutrophication in the Pearl River Estuary, South China. *Marine Pollution Bulletin*, 47(1–6), 30–36. [https://doi.org/10.1016/s0025-326x\(02\)00474-5](https://doi.org/10.1016/s0025-326x(02)00474-5)
- Ianiri, H. L., Shen, Y., Broek, T. A. B., & McCarthy, M. D. (2022). Bacterial sources and cycling dynamics of amino acids in high and low molecular weight dissolved organic nitrogen in the ocean. *Marine Chemistry*, 241, 104104. <https://doi.org/10.1016/j.marchem.2022.104104>
- Jiang, Z. Y., Wang, Y. S., Cheng, H., Sun, C. C., & Wu, M. L. (2015). Variation of phytoplankton community structure from the Pearl River Estuary to South China Sea. *Ecotoxicology*, 24(7–8), 1442–1449. <https://doi.org/10.1007/s10646-015-1494-9>
- Ke, S., Zhang, P., Ou, S., Zhang, J., Chen, J., & Zhang, J. (2022). Spatiotemporal nutrient patterns, composition, and implications for eutrophication mitigation in the Pearl River Estuary, China. *Estuarine, Coastal and Shelf Science*, 266, 107749. <https://doi.org/10.1016/j.ecss.2022.107749>
- Lawaetz, A. J., & Stedmon, C. A. (2009). Fluorescence intensity calibration using the Raman scatter peak of water. *Applied Spectroscopy*, 63(8), 936–940. <https://doi.org/10.1366/000370209788964548>
- Lee, S. A., Kim, T. H., & Kim, G. (2020). Tracing terrestrial versus marine sources of dissolved organic carbon in a coastal bay using stable carbon isotopes. *Biogeosciences*, 17(1), 135–144. <https://doi.org/10.5194/bg-17-135-2020>
- Li, D., Gan, J., Hui, R., Liu, Z., Yu, L., Lu, Z., & Dai, M. (2020). Vortex and biogeochemical dynamics for the hypoxia formation within the coastal transition zone off the Pearl River Estuary. *Journal of Geophysical Research: Oceans*, 125(8), e2020JC016178. <https://doi.org/10.1029/2020JC016178>
- Li, J., Chen, Z., Jing, Z., Zhou, L., Li, G., Ke, Z., et al. (2019). Synechococcus bloom in the Pearl River Estuary and adjacent coastal area—With special focus on flooding during wet seasons. *Science of the total environment*, 692, 769–783. <https://doi.org/10.1016/j.scitotenv.2019.07.088>
- Li, R. H., Liu, S. M., Li, Y. W., Zhang, G. L., Ren, J. L., & Zhang, J. (2014). Nutrient dynamics in tropical rivers, lagoons, and coastal ecosystems of eastern Hainan Island, South China Sea. *Biogeosciences*, 11(2), 481–506. <https://doi.org/10.5194/bg-11-481-2014>
- Li, Y., Song, G., Massicotte, P., Yang, F., Li, R., & Xie, H. (2019). Distribution, seasonality, and fluxes of dissolved organic matter in the Pearl River (Zhujiang) estuary, China. *Biogeosciences*, 16(13), 2751–2770. <https://doi.org/10.5194/bg-16-2751-2019>
- Liao, K. W., Hu, H. D., Ma, S. J., & Ren, H. Q. (2019). Effect of microbial activity and microbial community structure on the formation of dissolved organic nitrogen (DON) and bioavailable DON driven by low temperatures. *Water Research*, 159, 397–405. <https://doi.org/10.1016/j.watres.2019.04.049>
- Liu, Q., Liang, Y., Cai, W., Wang, K., Wang, J., & Yin, K. (2020). Changing riverine organic C:N ratios along the Pearl River: Implications for estuarine and coastal carbon cycles. *Science of the Total Environment*, 709, 136052. <https://doi.org/10.1016/j.scitotenv.2019.136052>
- Lu, D., Yang, N., Liang, S., Li, K., & Wang, X. (2016). Comparison of land-based sources with ambient estuarine concentrations of total dissolved nitrogen in Jiaozhou Bay (China). *Estuarine, Coastal and Shelf Science*, 180, 82–90. <https://doi.org/10.1016/j.ecss.2016.06.032>
- Lu, F.-H., Ni, H.-G., Liu, F., & Zeng, E. Y. (2009). Occurrence of nutrients in riverine runoff of the Pearl River Delta, South China. *Journal of Hydrology*, 376(1–2), 107–115. <https://doi.org/10.1016/j.jhydrol.2009.07.018>
- Lu, Z., & Gan, J. (2015). Controls of seasonal variability of phytoplankton blooms in the Pearl River Estuary. *Deep Sea Research Part II: Topical Studies in Oceanography*, 117, 86–96. <https://doi.org/10.1016/j.dsr2.2013.12.011>
- Lu, Z., Gan, J., Dai, M., Liu, H., & Zhao, X. (2018). Joint effects of extrinsic biophysical fluxes and intrinsic hydrodynamics on the formation of hypoxia west off the Pearl River Estuary. *Journal of Geophysical Research: Oceans*, 123(9), 6241–6259. <https://doi.org/10.1029/2018jc014199>
- Lusk, M. G., & Toor, G. S. (2016). Dissolved organic nitrogen in urban streams: Biodegradability and molecular composition studies. *Water Research*, 96, 225–235. <https://doi.org/10.1016/j.watres.2016.03.060>
- Ma, X., Johnson, K. B., Gu, B., Zhang, H., Li, G., Huang, X., & Xia, X. (2022). The in-situ release of algal bloom populations and the role of prokaryotic communities in their establishment and growth. *Water Research*, 219, 118565. <https://doi.org/10.1016/j.watres.2022.118565>
- McCallum, R., Eyre, B., Hyndes, G., Wells, N. S., Oakes, J. M., & Wells, N. S. (2021). Importance of internal dissolved organic nitrogen loading and cycling in a small and heavily modified coastal lagoon. *Biogeochemistry*, 155(2), 237–261. <https://doi.org/10.1007/s10533-021-00824-5>
- McClelland, J. W., & Valiela, I. (1998). Linking nitrogen in estuarine producers to land-derived sources. *Limnology & Oceanography*, 43(4), 577–585. <https://doi.org/10.4319/lno.1998.43.4.0577>
- Medeiros, P. M., Seidel, M., Ward, N. D., Carpenter, E. J., Gomes, H. R., Niggemann, J., et al. (2015). Fate of the Amazon River dissolved organic matter in the tropical Atlantic Ocean. *Global Biogeochemical Cycles*, 29(5), 677–690. <https://doi.org/10.1002/2015gb005115>
- Meng, F., Huang, G., Yang, X., Li, Z., Li, J., Cao, J., et al. (2013). Identifying the sources and fate of anthropogenically impacted dissolved organic matter (DOM) in urbanized rivers. *Water Research*, 47(14), 5027–5039. <https://doi.org/10.1016/j.watres.2013.05.043>
- Middelburg, J. J., & Nieuwenhuize, J. (2001). Nitrogen isotope tracing of dissolved inorganic nitrogen behaviour in tidal estuaries. *Estuarine, Coastal and Shelf Science*, 53(3), 385–391. <https://doi.org/10.1006/ecss.2001.0805>
- Murphy, K. R., Hambly, A., Singh, S., Henderson, R. K., Baker, A., Stuetz, R., & Khan, S. J. (2011). Organic matter fluorescence in municipal water recycling schemes: Toward a unified PARAFAC model. *Environmental Science & Technology*, 45(7), 2909–2916. <https://doi.org/10.1021/es103015e>

- Niu, L., van Gelder, P., Luo, X., Cai, H., Zhang, T., & Yang, Q. (2020). Implications of nutrient enrichment and related environmental impacts in the Pearl River Estuary, China: Characterizing the seasonal influence of riverine input. *Water*, *12*(11), 3245. <https://doi.org/10.3390/w12113245>
- Osburn, C. L., Handsel, L. T., Peierls, B. L., & Paerl, H. W. (2016). Predicting sources of dissolved organic nitrogen to an estuary from an agro-urban coastal watershed. *Environmental Science & Technology*, *50*(16), 8473–8484. <https://doi.org/10.1021/acs.est.6b00053>
- Paerl, H. W. (1997). Coastal eutrophication and harmful algal blooms: Importance of atmospheric deposition and groundwater as “new” nitrogen and other nutrient sources. *Limnology & Oceanography*, *42*(5part2), 1154–1165. https://doi.org/10.4319/lo.1997.42.5_part_2.1154
- Paerl, H. W. (2006). Assessing and managing nutrient-enhanced eutrophication in estuarine and coastal waters: Interactive effects of human and climatic perturbations. *Ecological Engineering*, *26*(1), 40–54. <https://doi.org/10.1016/j.ecoleng.2005.09.006>
- Pennino, M. J., Kaushal, S. S., Murthy, S. N., Blomquist, J. D., Cornwell, J. C., & Harris, L. A. (2016). Sources and transformations of anthropogenic nitrogen along an urban river–estuarine continuum. *Biogeosciences*, *13*(22), 6211–6228. <https://doi.org/10.5194/bg-13-6211-2016>
- Petrone, K. C., Richards, J. S., & Grierson, P. F. (2008). Bioavailability and composition of dissolved organic carbon and nitrogen in a near coastal catchment of south-western Australia. *Biogeochemistry*, *92*(1–2), 27–40. <https://doi.org/10.1007/s10533-008-9238-z>
- Qian, W., Gan, J., Liu, J., He, B., Lu, Z., Guo, X., et al. (2018). Current status of emerging hypoxia in a eutrophic estuary: The lower reach of the Pearl River Estuary, China. *Estuarine, Coastal and Shelf Science*, *205*, 58–67. <https://doi.org/10.1016/j.ecss.2018.03.004>
- Rabouille, C., Mackenzie, F. T., & Ver, L. M. (2001). Influence of the human perturbation on carbon, nitrogen, and oxygen biogeochemical cycles in the global coastal ocean. *Geochimica et Cosmochimica Acta*, *65*(21), 3615–3641. [https://doi.org/10.1016/S0016-7037\(01\)00760-8](https://doi.org/10.1016/S0016-7037(01)00760-8)
- Rath, A. R., Mitbavkar, S., & Anil, A. C. (2021). Response of the phytoplankton community to seasonal and spatial environmental conditions in the Haldia port ecosystem located in the tropical Hooghly River estuary. *Environmental Monitoring and Assessment*, *193*(9), 548. <https://doi.org/10.1007/s10661-021-09255-z>
- Seidel, M., Yager, P. L., Ward, N. D., Carpenter, E. J., Gomes, H. R., Krusche, A. V., et al. (2015). Molecular-level changes of dissolved organic matter along the Amazon River-to-ocean continuum. *Marine Chemistry*, *177*, 218–231. <https://doi.org/10.1016/j.marchem.2015.06.019>
- Sipler, R. E., & Bronk, D. A. (2015). Dynamics of dissolved organic nitrogen. In *Biogeochemistry of marine dissolved organic matter* (pp. 127–232). <https://doi.org/10.1016/b978-0-12-405940-5.00004-2>
- Statham, P. J. (2012). Nutrients in estuaries—An overview and the potential impacts of climate change. *Science of the Total Environment*, *434*, 213–227. <https://doi.org/10.1016/j.scitotenv.2011.09.088>
- Stedmon, C. A., & Bro, R. (2008). Characterizing dissolved organic matter fluorescence with parallel factor analysis: A tutorial. *Limnology and Oceanography: Methods*, *6*(11), 572–579. <https://doi.org/10.4319/lom.2008.6.572>
- Stedmon, C. A., Markager, S., & Bro, R. (2003). Tracing dissolved organic matter in aquatic environments using a new approach to fluorescence spectroscopy. *Marine Chemistry*, *82*(3–4), 239–254. [https://doi.org/10.1016/s0304-4203\(03\)00072-0](https://doi.org/10.1016/s0304-4203(03)00072-0)
- Strokal, M., Kroeze, C., Li, L., Luan, S., Wang, H., Yang, S., & Zhang, Y. (2015). Increasing dissolved nitrogen and phosphorus export by the Pearl River (Zhujiang): A modeling approach at the sub-basin scale to assess effective nutrient management. *Biogeochemistry*, *125*(2), 221–242. <https://doi.org/10.1007/s10533-015-0124-1>
- Strokal, M., Kroeze, C., Wang, M., & Ma, L. (2017). Reducing future river export of nutrients to coastal waters of China in optimistic scenarios. *Science of the Total Environment*, *579*, 517–528. <https://doi.org/10.1016/j.scitotenv.2016.11.065>
- Su, J. (2004). Overview of the South China Sea circulation and its influence on the coastal physical oceanography outside the Pearl River Estuary. *Continental Shelf Research*, *24*(16), 1745–1760. <https://doi.org/10.1016/j.csr.2004.06.005>
- Tao, W., Niu, L., Dong, Y., Fu, T., & Lou, Q. (2021). Nutrient pollution and its dynamic source-sink pattern in the Pearl River Estuary (South China). *Frontiers in Marine Science*, *8*, 1321. <https://doi.org/10.3389/fmars.2021.713907>
- Wang, B., Ming, X., Wei, Q., & Xie, L. (2018). A historical overview of coastal eutrophication in the China Seas. *Marine Pollution Bulletin*, *136*, 394–400. <https://doi.org/10.1016/j.marpolbul.2018.09.044>
- Wang, C., Lv, Y., & Li, Y. (2018). Riverine input of organic carbon and nitrogen in water-sediment system from the Yellow River estuary reach to the coastal zone of Bohai Sea, China. *Continental Shelf Research*, *157*, 1–9. <https://doi.org/10.1016/j.csr.2018.02.004>
- Wang, L., Zhang, X., Chen, S., Meng, F., Zhang, D., Liu, Y., et al. (2021). Spatial variation of dissolved organic nitrogen in Wuhan surface waters: Correlation with the occurrence of disinfection byproducts during the COVID-19 pandemic. *Water Research*, *198*, 117138. <https://doi.org/10.1016/j.watres.2021.117138>
- Wang, Q., Wang, X., Xiao, K., Zhang, Y., Luo, M., Zheng, C., & Li, H. (2021). Submarine groundwater discharge and associated nutrient fluxes in the Greater Bay Area, China revealed by radium and stable isotopes. *Geoscience Frontiers*, *12*(5), 101223. <https://doi.org/10.1016/j.gsf.2021.101223>
- Wang, X., Xiong, Y., Zheng, C., Li, H., Zhang, Y., Luo, M., et al. (2021). Radium and nitrogen isotopes tracing fluxes and sources of submarine groundwater discharge driven nitrate in an urbanized coastal area. *Science of the Total Environment*, *763*, 144616. <https://doi.org/10.1016/j.scitotenv.2020.144616>
- Wang, Y., Liu, D., Dong, Z., Di, B., & Shen, X. (2012). Temporal and spatial distributions of nutrients under the influence of human activities in Sishili Bay, northern Yellow Sea of China. *Marine Pollution Bulletin*, *64*(12), 2708–2719. <https://doi.org/10.1016/j.marpolbul.2012.09.024>
- Worsfold, P. J., Monbet, P., Tappin, A. D., Fitzsimons, M. F., Stiles, D. A., & McKelvie, I. D. (2008). Characterisation and quantification of organic phosphorus and organic nitrogen components in aquatic systems: A review. *Analytica Chimica Acta*, *624*(1), 37–58. <https://doi.org/10.1016/j.aca.2008.06.016>
- Wu, K., Dai, M., Li, X., Meng, F., Chen, J., & Lin, J. (2017). Dynamics and production of dissolved organic carbon in a large continental shelf system under the influence of both river plume and coastal upwelling. *Limnology & Oceanography*, *62*(3), 973–988. <https://doi.org/10.1002/lno.10479>
- Wu, M., Hong, Y., Yin, J., Dong, J., & Wang, Y. (2016). Evolution of the sink and source of dissolved inorganic nitrogen with salinity as a tracer during summer in the Pearl River Estuary. *Scientific Report*, *6*(1), 36638. <https://doi.org/10.1038/srep36638>
- Xie, M., Chen, M., & Wang, W. (2018). Spatial and temporal variations of bulk and colloidal dissolved organic matter in a large anthropogenically perturbed estuary. *Environmental Pollution*, *243*, 1528–1538. <https://doi.org/10.1016/j.envpol.2018.09.119>
- Xu, S., Liu, Y., Fan, J., Xiao, Y., Qi, Z., & Lakshmikanandan, M. (2022). Impact of salinity variation and silicate distribution on phytoplankton community composition in Pearl River estuary, China. *Ecology and Hydrobiology*, *22*(3), 466–475. <https://doi.org/10.1016/j.ecohyd.2022.01.004>
- Xu, Y., Zhang, T., & Zhou, J. (2019). Historical occurrence of algal blooms in the northern Beibu Gulf of China and implications for future trends. *Frontiers in Microbiology*, *10*, 451. <https://doi.org/10.3389/fmicb.2019.00451>
- Yan, X., Wan, X. S., Liu, L., Xu, M. N., Tan, E., Zheng, Z., et al. (2019). Biogeochemical dynamics in a eutrophic tidal estuary revealed by isotopic compositions of multiple nitrogen species. *Journal of Geophysical Research: Biogeosciences*, *124*(7), 1849–1864. <https://doi.org/10.1029/2018JG004959>

- Ye, F., Guo, W., Wei, G., & Jia, G. (2018). The sources and transformations of dissolved organic matter in the Pearl River Estuary, China, as revealed by stable isotopes. *Journal of Geophysical Research: Oceans*, *123*(9), 6893–6908. <https://doi.org/10.1029/2018jc014004>
- Zhang, Q., Wang, Y., Song, M., Wang, J., Ji, N., Liu, C., et al. (2022). First record of a Takayama bloom in Haizhou Bay in response to dissolved organic nitrogen and phosphorus. *Marine Pollution Bulletin*, *178*, 113572. <https://doi.org/10.1016/j.marpolbul.2022.113572>
- Zhou, Y., He, D., He, C., Li, P., Fan, D., Wang, A., et al. (2021). Spatial changes in molecular composition of dissolved organic matter in the Yangtze River Estuary: Implications for the seaward transport of estuarine DOM. *Science of the Total Environment*, *759*, 143531. <https://doi.org/10.1016/j.scitotenv.2020.143531>
- Zhou, Z., Kong, F., Zhang, Q., Gao, Y., Koch, F., Gobler, C. J., et al. (2023). Brown tides linked to the unique nutrient profile in coastal waters of Qinhuangdao, China. *Environmental Research*, *216*, 114459. <https://doi.org/10.1016/j.envres.2022.114459>

References From the Supporting Information

- Murphy, K. R., Stedmon, C. A., Wenig, P., & Bro, R. (2014). OpenFluor—An online spectral library of auto-fluorescence by organic compounds in the environment. *Analytical Methods*, *6*, 4. <https://doi.org/10.1039/c3ay41935e>
- Tang, Y., Wang, M., Liu, Q., Hu, Z., Zhang, J., Shi, T., et al. (2022). Ecological carrying capacity and sustainability assessment for coastal zones: A novel framework based on spatial scene and three-dimensional ecological footprint model. *Ecological Modelling*, *466*, 109881. <https://doi.org/10.1016/j.ecolmodel.2022.109881>
- Wang, X., Li, H., Yang, J., Zheng, C., Zhang, Y., An, A., et al. (2017). Nutrient inputs through submarine groundwater discharge in an embayment: A radon investigation in Daya Bay, China. *Journal of Hydrology*, *551*, 784–792. <https://doi.org/10.1016/j.jhydrol.2017.02.036>